Edge-directed [(M₂)₂L₄] tetragonal metal–organic polyhedra decorated using a square paddle-wheel secondary building unit†

M. Jaya Prakash, Minhak Oh, Xinfang Liu, Kwi Nam Han, Gi Hun Seong and Myoung Soo Lah*

A general strategy was developed for edge-directed self-assembly of tetragonal metal–organic polyhedra (MOPs) having a C_4 symmetry $Cu^{II}_2(COO)_4$ paddle-wheel as a secondary building unit, using C_2 symmetric dicarboxylic ligands as pincer-type primary building units.

Metal–organic polyhedra (MOPs) are a class of metal–organic systems developed for various potential applications including recognition and storage,[1] catalysis,[2] delivery, and synthetic membranes for ionic channels.[3] MOPs of various high symmetries have been reported, such as O, T, or I symmetries.[4] The MOPs are developed by two strategies, edge-directed linear components connected at the corners[5] and face-directed facial components connected at the edges[6] or at the corners.[7] Some MOPs with tetragonal symmetry have been reported in the literature, where C_2 symmetric bidentate ligands with Cu^{II}, Pd^{II}, Co^{II}, Pd^{II} or Mn^{II} metal ions to form edge-directed[8,9] or C_4 symmetric tetradentate ligand with Rh^{IV}_2 to form face-directed tetragonal systems.[10] Even though several highly symmetric decorated MOPs, such as cuboctahedral[11] or octahedral[12] cages, have been prepared using a secondary building unit approach, there are only a few reports of low symmetry decorated cage systems, such as an augmented tetragonal MOP.[9c,10]

Here we report preparations of tetragonal MOPs decorated with a $Cu_2(COO)_4$ paddle-wheel secondary building unit (SBU), where primary building units, C_2 symmetric pincer-type ditopic ligands, self-assemble with Cu^{II} to generate a C_4 symmetric $Cu_2(COO)_4$ paddle-wheel as a tetratopic SBU (Fig. 1a). Each ligand occupying the edge of the tetragonal cage connects to two square-planar $Cu_2(COO)_4$ paddle-wheels to form an augmented tetragonal MOP.

A solvothermal reaction of 3,3′-[1,3-benzenediyldi-(ethynyl)]dibenzoic acid (H_2L^1) with $Cu(NO_3)_2\cdot3H_2O$ in N,N'-dimethylformamide (DMF) resulted in the mixture of crystals having two slightly different morphologies, block-shaped greenish-blue crystals as a pseudo-polymorph (MOP-**1a**) as a major form and rectangle-shaped blue crystals as another pseudo-polymorph (MOP-**1b**) as a minor form, which were

separated manually under an optical microscope (Fig. S1†). MOP-**1a**, [(Cu₂)₂L¹₄(DMF)₄], is composed of individual tetragonal-shaped cages, and each cage is composed of four bidentate ligands and two $Cu_2(COO)_4$ paddle-wheel moieties (Fig. 1b).‡ The two carboxylate groups in the ligand are on the same side to serve as a pincer-type ligand, and the ligand serves as an edge of the tetragonal cage. In MOP-**1a**, four ligands are connected with two paddle-wheel moieties, with each paddle-wheel moiety coordinated with two DMF solvent molecules. The outer dimension of the cage between the phenyl residues of the ligands on opposite sides is ∼24 Å, and the dimension of the cage between the metal ions of the paddle-wheel SBUs is ∼17 Å (Fig. S2†). The window of the cage formed by two ligands is ∼7.1 Å wide and ∼6.4 Å high (Fig. S3†). The dimensions of the inner cavity of the MOP are ∼11 Å across the phenyl groups and ∼5 Å between the metal ions of the paddle-wheel SBUs (Fig. S4†).

Two different types of inter-cage π–π stacking interactions have been observed (Fig. S5 and Table S4†). Type-I interaction occurs bilaterally between the terminal phenyl groups of the ligands; type-II interaction also occurs bilaterally, but between the terminal phenyl group and the ethynyl group of the ligands. The alternating interactions between the cages lead to 1D chains (Fig. S6†), which in turn interact with neighboring chains *via* van der Waals interactions only to form a 2D sheet (Fig. S7†); the 2D sheets are further stacked into a 3D packing structure (Fig. S8†). Even though the tetragonal MOPs in the crystal are compactly arranged, the rigidity of the ligands in the corresponding MOP and the intercage π–π stacking interactions between the MOPs render solvent space in the crystal packing structure. In the crystal structure of MOP-**1a**, the solvent cavity volume of 1117 Å³ per unit cell represents ∼20.6% of the whole crystal volume.
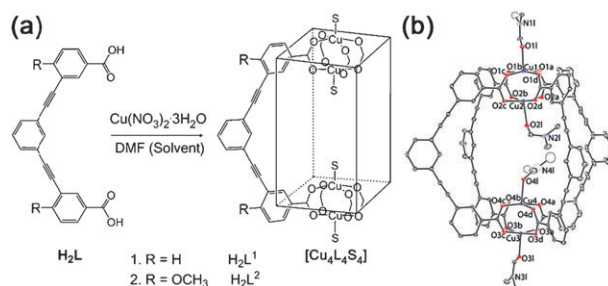
Fig. 1 (a) A reaction scheme for the self-assembly of augmented tetragonal MOPs. (b) An ORTEP representation of the one cage unit of MOP-**1a** with 20% of thermal ellipsoid probability displacement. Hydrogen atoms were omitted for clarity.

Department of Chemistry and Applied Chemistry, Hanyang University, Ansan, Kyunggi-do, 426-791, Korea. E-mail: mslah@hanyang.ac.kr; Fax: +82 31 436 8100; Tel: +82 31 400 5496

Similar to MOP-**1a**, the crystals of MOP-**1b** ([(Cu₂)₂L¹₄(DMF)₄]) are also composed of isostructural tetragonal-shaped cages in crystallographic inversion centers (Fig. S9†). The cage itself in MOP-**1b** is chemically identical to that of MOP-**1a** but has a higher symmetry imposed by the crystallographic restraint.

The cages in MOP-**1b** are also involved in an inter-cage π–π stacking interaction to form 1D chains, where only the type-I interaction is utilized (Fig. S10 and Table S4†). The 1D chains in MOP-**1b** interact with the neighboring chains to form 2D sheets *via* van der Waals interactions (Fig. S11(a)†), and then form a 3D packing structure (Fig. S11(b)†). A slightly different packing in the MOP-**1b** leads to the slightly different solvent cavity volume of 3179 Å³ per unit cell, which represents ∼26.6% of the whole crystal volume.

The powder X-ray diffraction (PXRD) pattern of the bulk sample of MOP-**1a** resembles the simulated pattern obtained from the single-crystal structure of MOP-**1a** (Fig. S12†). The activated sample of MOP-**1a**, which was prepared by soaking in DMF, methanol, and methylene chloride and then by vacuum-drying overnight at 90 °C, showed a PXRD pattern different from that of the as-synthesized material. The substitution of the ligated solvent DMF to methanol and/or the removal of the guest solvents from the solvent cavity lead to a structural transformation of MOP-**1a** to another polymorphic form. This transformation is irreversible: the PXRD pattern of the activated sample resoaked in fresh DMF solvent was completely different from those of both the as-synthesized and activated samples.

The PXRD pattern of the bulk MOP-**1b** was different from that of bulk MOP-**1a**, which confirmed the packing of the MOPs in the two pseudo-polymorphs differed. The PXRD pattern of the bulk MOP-**1b** matched the simulated PXRD pattern from the single crystal structure of MOP-**1b** with [010] preferred sample orientation rather than with random sample orientation (Fig. S13†).

The sorption behaviors of the activated MOP-**1a**, which had been vacuum-dried at 120 °C after soaking in DMF, methanol, and methylene chloride, have been studied for N₂ and H₂ at 77 K and for CO₂ and CH₄ at 195 K (Fig. 2). The N₂ sorption isotherm did not indicate any appreciable amount of adsorption, which strongly suggested that the activated MOP-**1a** did not have any accessible pore for N₂ gas. The H₂ and CH₄ sorption behaviors were also similar to N₂, and only a very small amount of gas sorption was observed. However, the CO₂ sorption isotherm was type-1 with 347 cm³ g⁻¹ capacity at 195 K and 1 bar. We speculate that the activation of MOP-**1a** might lead to a structure having an accessible pore with a pore window that only allows the CO₂ gas molecule. We speculate that even though the window size of the tetragonal cage unit is large enough to allow all the gas molecules to be adsorbed, the activation of MOP-**1a** might lead to a packing structure having the window of the tetragonal cage partially blocked by adjacent cages and the adjusted window size only suitable to CO₂ gas molecule to penetrate.

The sorption behaviors of the activated MOP-**1b** (Fig. S14†) are similar to those of the activated MOP-**1a**. Although the PXRD pattern of the as-synthesized MOP-**1b** was different
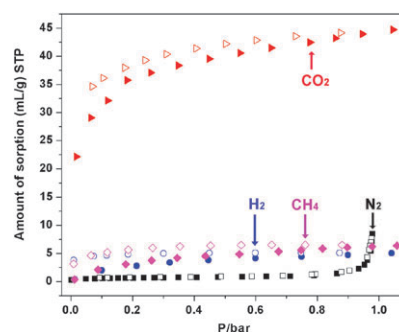
Fig. 2 Gas sorption isotherms of MOP-**1a**. Filled symbols represent adsorption isotherms, and empty symbols represent desorption isotherms.

from that of the as-synthesized MOP-**1a**, there is some similarity between the PXRD pattern of the activated MOP-**1b** and that of the activated MOP-**1a** (Fig. S15†), which suggests that both the structures transform to the unknown but similar polymorphic form in their packing structures when they are activated, which might lead to the similar gas sorption behaviors.

Because of the limited solubility of both MOP-**1a** and MOP-**1b** in aqueous and ordinary organic solvents, we have introduced the methoxy group into the ligand to improve the solubility of the MOPs. We prepared another similar kind of tetragonal-cage MOP-**2**, ([(Cu₂)₂L²₄(DMF)₄]), using 3,3′-[1,3-benzenediyldi(ethynyl)]bis(4-methoxy)benzoic acid (H₂L²) as a methoxy-derivatized ligand. The solvothermal reaction of H₂L² with Cu(NO₃)₂·3H₂O in the DMF + CH₃CN (1:1) solvent mixture resulted in blue, block-shaped crystals. The tetragonal cage in the MOP-**2** is very similar to those described in the MOP-**1a** and MOP-**1b** structures, except that there are two additional methoxy groups per ligand (Fig. S16†). As in MOP-**1a** and MOP-**1b**, a type-I inter-cage π–π stacking interaction between the tetragonal cages in the MOP-**2** structure leads to 1D chains (Fig. S17 and Table S4†). The 1D chains interact with the neighboring chains *via* a type-III inter-cage π–π stacking interaction to form a 2D sheet (Fig. S18†) based on the two different kinds of inter-cage π–π stacking interactions, and 3D packing is accomplished *via* weak van der Waals interaction between the 2D sheets (Fig. S19†). The solvent cavity of the MOP-**2** crystal takes 39.1% of the whole crystal volume (2884 Å³ per unit cell), which is a significantly larger proportion than in MOP-**1a** and MOP-**1b** crystals. The phase purity of MOP-**2** was confirmed by comparing the PXRD pattern of the bulk sample with that simulated from the single crystal structure (Fig. S20†). The activation of MOP-**2** causes a loss in crystallinity and leads to the gas sorption behavior of the nonporous material.

The solution integrity of MOP-**2** could be investigated using nuclear magnetic resonance (NMR) spectroscopy in DMF solvent, because the solubility of the complex could be improved by the introduction of methoxy groups into the ligand. MOP-**2** in d₇-DMF gave broad peaks in the ¹H-NMR spectrum because of the electronic effect of the paramagnetic Cuᴵᴵ ion, which contrasts the sharp peaks in the ¹H-NMR spectrum of the free ligand (Fig. S21†). Two pairs of singlet and multiplet peaks between 2.7 and 3 ppm and a peak at

around 8.0 ppm were attributable to DMF molecules in two different environments, which indicated that the ligated DMF molecules were not replaced by the solvent DMF molecules in the NMR time scale. Similar behavior has been observed for other Cu^{II} complexes, such as [Cu$^{II}_2$(Indo)$_4$(DMF)$_2$] (HIndo: Indomethacin [1-(4-chlorobenzoyl)-5-methoxy-2-methyl-1H-indole-3-acetic acid), containing a Cu$_2$(COO)$_4$ paddle-wheel unit with ligated DMF molecules.[13] Even though there are six chemically different aromatic protons and methyl protons of the methoxy group in the complex, only three broad peaks were observed for the aromatic protons at 9.66, 8.30 and 7.33 ppm, and one for the methyl protons of the methoxy group at 3.65 ppm. The reduction in the number of observed peaks around the aromatic region might be attributed to the extreme broadening of some proton peaks by the influence of paramagnetic Cu^{II} centers.

Although the NMR spectrum of MOP-**2** indicated that the ligand and some solvent DMF molecules were engaged with the Cu$_2$(COO)$_4$ paddle-wheel unit, the information regarding the solution integrity of MOP-**2** was limited, and we have taken the atomic force microscopy (AFM) image of MOP-**2** in DMF. Discrete MOP molecules were observed as individual particles on a mica sheet with an average height of ∼1.8 nm, which is smaller than the approximate dimension of the MOP from single crystal structure analysis, 2.4 nm in diameter (Fig. S22†). Height contraction of a similar extent (∼30%) was observed for the other MOPs in the AFM images, in the tapping mode of scanning the samples.[7b,c]

We have demonstrated the preparation of the augmented tetragonal MOPs using pincer-type C_2 symmetric ditopic dicarboxylic ligands. The pincer-type ligands self-assembled with Cu^{II} ions to form tetragonal MOPs having two square-planar tetratopic Cu$_2$(COO)$_4$ paddle-wheels as a secondary building unit and the rigid bent linkage moieties of the ligands as edges of the tetragonal cage. Depending on the crystal structures, the tetragonal MOPs are differently arranged by use of various kinds and combinations of π–π stacking interactions between the conjugated moieties of the ligands in addition to van der Waals interactions. The different packings lead to different proportions of solvent cavities in the crystal structures. The guest removal from the cavities caused irreversible structural transformations to an unknown crystalline or amorphous phase. The microporosity of the activated MOPs was demonstrated in MOP-**1a** and MOP-**1b**, whereas MOP-**2** did not show any gas sorption. The solution integrity of MOP-**2**, which has improved the solubility property compared with MOP-**1a** and MOP-**1b** with no methoxy residues, was characterized using NMR spectroscopy and further supported by AFM studies.

Notes and references

‡ Crystal data for MOP-**1a**: [(Cu$_2$)$_2$L$^1_4$(DMF)$_4$] (C$_{114}$H$_{90}$N$_6$O$_{22}$Cu$_4$), fw = 2150.08 g mol^{-1}, triclinic, space group $P\bar{1}$, a = 17.475(4) Å, b = 18.723(4) Å, c = 18.786(4) Å, α = 82.05(3)°, β = 62.82(3)°, γ = 87.67(3)°, V = 5414.3(19) Å^3, Z = 2, μ (synchrotron,

λ = 0.72999 Å) = 0.847 mm^{-1}, 67393 reflections were collected, 33839 were unique [R_{int} = 0.0571]. R1($wR2$) = 0.0830 (0.2427) for 27707 reflections [$I > 2\sigma(I)$], R1($wR2$) = 0.0911 (0.2534) for all reflections. Crystal data for MOP-**1b**: [(Cu$_2$)L$^1_2$(DMF)$_2$] (C$_{54}$H$_{38}$N$_2$O$_{10}$Cu$_2$), fw = 1001.94 g mol^{-1}, monoclinic, space group $C2/c$, a = 11.245(2) Å, b = 37.235(7) Å, c = 28.875(6) Å, β = 98.01(3)°, V = 11972(4) Å^3, Z = 8, μ (synchrotron, λ = 0.75000 Å) = 0.766 mm^{-1}, 53617 reflections were collected, 14391 were unique [R_{int} = 0.0864]. R1($wR2$) = 0.0815 (0.2357) for 12173 reflections [$I > 2\sigma(I)$], R1($wR2$) = 0.0900 (0.2452) for all reflections. Crystal data for MOP-**2**: [(Cu$_2$)$_2$L$^2_2$(DMF)$_2$]·3.25DMF·2.25MeCN·0.5H$_2$O (C$_{72.25}$H$_{76.50}$N$_{7.50}$O$_{17.75}$Cu$_2$), fw = 1460.99 g mol^{-1}, monoclinic, space group $P2_1/n$, a = 13.187(3) Å, b = 29.985(6) Å, c = 18.713(4) Å, β = 93.93(3)°, V = 7382(3) Å^3, Z = 4, μ (synchrotron, λ = 0.75000 Å) = 0.648 mm^{-1}, 61282 reflections were collected, 19718 were unique [R_{int} = 0.0464]. R1($wR2$) = 0.0716 (0.2019) for 16424 reflections [$I > 2\sigma(I)$], R1($wR2$) = 0.0829 (0.2153) for all reflections.

1 (a) S. Tashiro, M. Tominaga, M. Kawano, B. Therrien, T. Ozeki and M. Fujita, *J. Am. Chem. Soc.*, 2005, **127**, 4546; (b) A. V. Davis and K. N. Raymond, *J. Am. Chem. Soc.*, 2005, **127**, 7912; (c) P. Mal, B. Breiner, K. Rissanen and J. R. Nitschke, *Science*, 2009, **324**, 1697.

2 (a) M. D. Pluth, R. G. Bergman and K. N. Raymond, *Science*, 2007, **316**, 85; (b) M. Yoshizawa, M. Tamura and M. Fujita, *Science*, 2006, **312**, 251.

3 M. Jung, H. Kim, K. Baek and K. Kim, *Angew. Chem., Int. Ed.*, 2008, **47**, 5755.

4 S. R. Seidel and P. J. Stang, *Acc. Chem. Res.*, 2002, **35**, 972.

5 (a) D. L. Caulder, R. E. Powers, T. N. Parac and K. N. Raymond, *Angew. Chem., Int. Ed.*, 1998, **37**, 1840; (b) M. Tominaga, K. Suzuki, M. Kawano, T. Kusukawa, T. Ozeki, S. Sakamoto, K. Yamaguchi and M. Fujita, *Angew. Chem., Int. Ed.*, 2004, **43**, 5621; (c) Y. Liu, V. C. Kravtsov, D. A. Beauchamp, J. F. Eubank and M. Eddaoudi, *J. Am. Chem. Soc.*, 2005, **127**, 7266.

6 (a) N. Takeda, K. Umemoto, K. Yamaguchi and M. Fujita, *Nature*, 1999, **398**, 794; (b) K. Umemoto, H. Tsukui, T. Kusukawa, K. Biradha and M. Fujita, *Angew. Chem., Int. Ed.*, 2001, **40**, 2620; (c) B. Olenyuk, J. A. Whiteford, A. Fechtenkotter and P. J. Stang, *Nature*, 1999, **398**, 796.

7 (a) C. Brückner, R. E. Powers and K. N. Raymond, *Angew. Chem., Int. Ed.*, 1998, **37**, 1837; (b) D. Moon, S. Kang, J. Park, K. Lee, R. P. John, H. Won, G. H. Seong, Y. S. Kim, G. H. Kim, H. Rhee and M. S. Lah, *J. Am. Chem. Soc.*, 2006, **128**, 3530; (c) J. Park, S. Hong, D. Moon, M. Park, K. Lee, S. Kang, Y. Zou, R. P. John, G. H. Kim and M. S. Lah, *Inorg. Chem.*, 2007, **46**, 10208; (d) T. K. Ronson, J. Fisher, L. P. Harding and M. J. Hardie, *Angew. Chem., Int. Ed.*, 2007, **46**, 9086; (e) Z. Lu, C. B. Knobler, H. Furukawa, B. Wang, G. Liu and O. M. Yaghi, *J. Am. Chem. Soc.*, 2009, **131**, 12532.

8 (a) L. J. Barbour, G. W. Orr and J. L. Atwood, *Nature*, 1998, **393**, 671; (b) D. A. McMorran and P. J. Steel, *Angew. Chem., Int. Ed.*, 1998, **37**, 3295; (c) N. L. S. Yue, D. J. Eisler, M. C. Jennings and R. J. Puddephatt, *Inorg. Chem.*, 2004, **43**, 7671; (d) Z.-M. Liu, Y. Liu, S.-R. Zheng, Z.-Q. Yu, M. Pan and C.-Y. Su, *Inorg. Chem.*, 2007, **46**, 5814; (e) B. Wu, D. Yuan, B. Lou, L. Han, C. Liu, C. Zhang and M. Hong, *Inorg. Chem.*, 2005, **44**, 9175.

9 (a) C.-Y. Su, Y.-P. Cai, C.-L. Chen, M. D. Smith, W. Kaim and H.-C. Z. Loye, *J. Am. Chem. Soc.*, 2003, **125**, 8595; (b) C.-Y. Su, Y.-P. Cai, C.-L. Chen, H.-X. Zhang and B.-S. Kang, *J. Chem. Soc., Dalton Trans.*, 2001, 359; (c) F. Dai, H. He, A. Xie, G. Chu, D. Sun and Y. Ke, *CrystEngComm*, 2009, **11**, 47.

10 F. A. Cotton, P. Lei, C. Lin, C. A. Murillo, X. Wang, S.-Y. Yu and Z.-X. Zhang, *J. Am. Chem. Soc.*, 2004, **126**, 1518.

11 (a) M. Eddaoudi, J. Kim, J. B. Wachter, H. K. Chae, M. O'Keeffe and O. M. Yaghi, *J. Am. Chem. Soc.*, 2001, **123**, 4368; (b) H. Furukawa, J. Kim, K. E. Plass and O. M. Yaghi, *J. Am. Chem. Soc.*, 2006, **128**, 8398; (c) H. Furukawa, J. Kim, N. W. Ockwig, M. O'Keeffe and O. M. Yaghi, *J. Am. Chem. Soc.*, 2008, **130**, 11650.

12 (a) Z. Ni, A. Yassar, T. Antoun and O. M. Yaghi, *J. Am. Chem. Soc.*, 2005, **127**, 12752; (b) M. J. Prakash, Y. Zou, S. Hong, M. Park, M.-P. N. Bui, G. H. Seong and M. S. Lah, *Inorg. Chem.*, 2009, **48**, 1281.

13 S. Ramadan, T. W. Hambley, B. J. Kennedy and P. A. Lay, *Inorg. Chem.*, 2004, **43**, 2943.